Communications in Physics, Vol. 34, No. 1 (2024), pp. 19-29
DOI: https://doi.org/10.15625/0868-3166/19163

Highly sensitive refractive index sensing based on nanostructured porous silicon interferometers

Nguyen Thuy Van[1,2,†], **Pham Thanh Son**[1], **Pham Thanh Binh**[1], **Vu Duc Chinh**[1,2], **Hoang Thi Hong Cam**[3], **Do Thuy Chi**[4], **Nguyen Anh Tuan**[4], **Bui Huy**[1,2] **and Pham Van Hoi**[1,2]

[1]*Institute of Materials Science, Vietnam Academy of Science and Technology, 18 Hoang Quoc Viet, 10000 Hanoi, Vietnam*

[2]*Graduate of University of Science and Technology, Vietnam Academy of Science and Technology, 18 Hoang Quoc Viet, 10000 Hanoi, Vietnam*

[3]*University of Science and Technology of Hanoi, Vietnam Academy of Science and Technology, 18 Hoang Quoc Viet, 10000 Hanoi, Vietnam*

[4]*Thai Nguyen University of Education, Thai Nguyen University, 20 Luong Ngoc Quyen, 250000 Thai Nguyen, Vietnam*

E-mail: †vannt@ims.vast.ac.vn

Received 12 October 2023; *Accepted for publication 28 December 2023*
Published 05 February 2024

Abstract. *In this study, we present the experimental evidence demonstrating the utility of electrical double layer (EDL)-induced ion accumulation, using sodium (Na^+) ion in water as a model substance, on a negatively charged nanostructured surface, specifically thermally grown silicon dioxide (SiO_2). This novel approach, termed Ion Surface Accumulation (ISA), aims to enhance the performance of nanostructured porous silicon (PSi) interferometers in optical refractometric applications. The experimental results show that the electrical double layer-induced ion surface accumulation (EDL-ISA) on oxidized PSi interferometers enables remarkable amplification of the interferometer output signal (the spectral interferogram), even when the bulk refractive index variation is below 10^{-3} RIU. This substantial signal enhancement translates into an increase in sensitivity of up to two orders of magnitude, facilitating the reliable measurement of refractive index variations with both a detection limit (DL) and resolution (R) as low as 10^{-4} RIU. This achievement elevates the performance of PSi interferometers in photonics and plasmonics-based refractive index platforms.*

Keywords: porous silicon; chemical sensor; metal ions.

Classification numbers: 07.07.Df; 81.05.Rm.

1. Introduction

Porous silicon (PSi) structures are formed in silicon by electrochemical anodization in a hydrofluoric acid (HF) solution [1]. Through precise control of formation conditions include HF conditions, current density and anodization time, pore diameters ranging from 2 nm to a few micrometers can be achieved. Recently, there has been a growing interest in utilizing PSi structures for refractive index optical sensors due to their potential for creating highly sensitive and compact refractometers [2–6]. The primary advantages of PSi include a high specific area of 200-300 m^2/cm^3, which accommodates a large number of molecules, thereby increasing the interaction between the electromagnetic field and the molecules of interest and improving sensitivity. Additionally, PSi preparation involves a single non-patterned electrochemical etching step, resulting in a low cost of \$0.01 per 8-inch silicon wafer [7]. Compared to other miniaturized photonic platforms [8], PSi has the distinct inherent capability to selectively filter out objects with dimensions larger than or similar to the pore size, mitigating potential interference and artifacts during real-field analysis [9–11].

This study proposes a novel approach using a facile fabrication method to enhance the sensitivity of PSi interferometers for highly-sensitive refractive index sensing. This enhancement is achieved through the utilization of an electrical double layer (EDL), which induces the accumulation of charged ions, i.e., Na^+ ions in water, onto a nanostructured surface characterized by a negative charge. This surface is specifically composed of thermally grown silicon dioxide and is referred to as Ion Surface Accumulation (ISA). Furthermore, through a comprehensive experimental analysis combined with an effective theoretical model, we demonstrate that the EDL-ISA technique significantly amplifies the output signal, represented as a spectral interferogram, of an oxidized PSi interferometer. This enhancement occurs particularly when there is a minor fluctuation in the bulk refractive index of the infiltrating solution, specifically when the variation is below 10^{-3} refractive index units (RIU), equivalent to NaCl concentration below 3%. Consequently, this advancement results in a remarkable improvement in sensitivity, up to two orders of magnitude, within the refractive index range of 10^{-3} to 10^{-4} RIU. Similar levels of sensitivity are achieved in these advanced platforms through more complex structures that come with significantly higher costs [12, 13].

The significant enhancement in sensitivity achieved through the proposed EDL-ISA approach enables the PSi interferometer, with a thickness of only 3 μm, to achieve a detection limit and resolution of approximately 10^{-4} RIU, equivalent to a NaCl concentration of about 1%. These findings effectively narrow the performance gap between PSi interferometers and established refractometric platforms such as plasmonics, ring resonators, and optical waveguides.

2. Experiment

The study involved the creation of PSi through electrochemical etching of boron-doped (100) p-type monocrystalline silicon wafers with a resistivity range of 0.01÷0.03 Ωcm. The etching process was carried out in a mixture consisting of HF and ethanol electrolyte solution with HF 48% wt. and absolute ethanol in a 1:2 volumetric ratio. The as-fabricated PSi interferometers undergo thermal oxidation in an ambient pressure furnace at 500˚C for 2 hours to form silicon dioxide layer for refractive index sensor application. The PSi samples were subjected to morphological and structural analysis using a field-emission scanning electron microscope (FESEM,

Hitachi S-4800, Hitachi, Tokyo, Japan). Moreover, the reflection spectra of the PSi samples were obtained at room temperature using a spectrometer (USB-4000, Ocean Optics) and a halogen light source (HL-2000 Ocean Optics) in the wavelength range 400 – 1000 nm.

The optofluidic experimental setup for reflection measurement on PSi interferometers is presented in Fig. 1. The PSi sample is placed in a Teflon flow cell with a volume of 100 μL and a transparent sapphire window that seals the chamber from the top. The flow cell is connected to a syringe pump that operates in withdraw mode, allowing solutions under test to be injected into the flow cell at a flow rate of 25 μL/min. The spectrometer is used to record the change in the reflectance spectrum of the sample as the analyte concentration is varied. After each measurement, the analytical solution is removed completely using deionized water. The refractive index sensor based on PSi interferometer relies on EDL-ISA effect. The silicon dioxide layer after thermal treatment acts as the negative surface charge, thus, attracts the positive ions to create a neutral charge surface due to chemical interactions. In addition, there exists a large number of hollow pillars which provide more space for the positive ions to reside. The higher accumulation of positive ions results in the increase of the effective refractive index of PSi layer which leads to the wavelength shift at the low concentration of analytical substances.

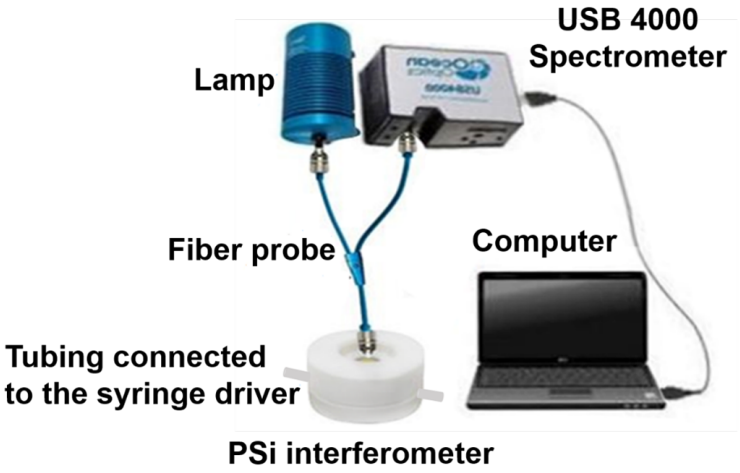

Fig. 1. Optofluidic experimental setup for reflection measurement on PSi interferometers.

3. Results and Discussion

Figure 2a presents a representative top-view scanning electron microscope (SEM) image of the PSi sensing layer. The image illustrates the presence of uniformly distributed pores with nearly circular shapes. In Fig. 2b, a cross-sectional SEM image of the PSi layer is displayed, revealing a thickness of approximately 2.8 μm and consisting of straight mesopores. To determine the size distribution of the pores, SEM image processing was performed using ImageJ software. The analysis showed that the pores ranged in size from 15 to 50 nm, with the highest frequency of pore sizes falling within the range of 20 to 25 nm, as depicted in Fig. 2c. Additionally, Fig. 2d

showcases the reflectance spectrum of the PSi structure, which exhibits multiple peaks resembling interference fringes in the wavelength range of 400 to 1000 nm.

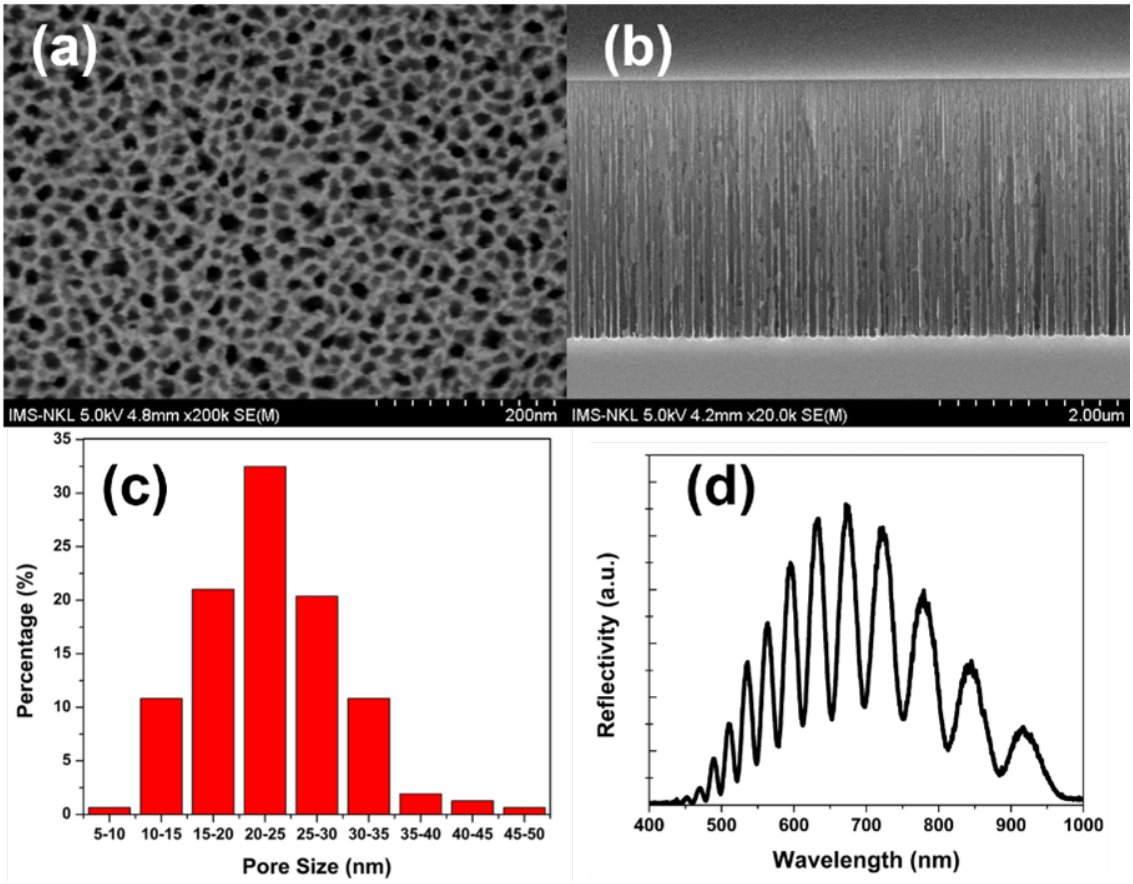

Fig. 2. SEM images of the PSi structure obtained from the etching process for 2 min at a current density of 50 mA.cm^{-1}: a) surface morphology, b) cross-section, c) pore size distribution, and d) reflectance spectrum of PSi.

The PSi samples are subjected to thermal oxidation in an ambient pressure furnace at 500˚C for 2 hours before being utilized as refractometric sensors. This process serves two primary purposes: first, to prevent uncontrolled oxidation of PSi in water-based solutions at room temperature, and second, to enhance the infiltration of water-based solutions containing Na^+Cl^- ion pair within the PSi structure. The stability of silicon dioxide in neutral or slightly acidic solutions, such as the deionized water (DIW)-based NaCl solution used in this study (with a pH ~ 5.5), is a contributing factor [14]. In addition, silicon dioxide exhibits hydrophilic properties, as evidenced by the decrease in contact angle from 110˚C for silicon to 13.5˚C for silicon dioxide [15].

The oxidation of PSi is confirmed through the Fast Fourier Transform (FFT) analysis of the reflection spectra collected in the air before (black trace) and after (red trace) the thermal oxidation, as shown in Fig. 3a. It is noteworthy that a discernible blue shift in the effective optical

thickness (EOT = $2n_{eff}d$, where n_{eff} and d represent the effective refractive index and the thickness of the porous medium, respectively) is observed following oxidation. Fig. 3b shows that the EOT shift changes from approximately 7030 nm for the as-etched PSi (black trace) to around 6491 nm for the oxidized PSi. This shift is attributed to the partial conversion of silicon to silicon dioxide. The alteration in EOT signifies a thin oxide layer within the inner section of the pores, resulting in a minor reduction in pore diameter and, consequently, causing a blue shift of the EOT [16].

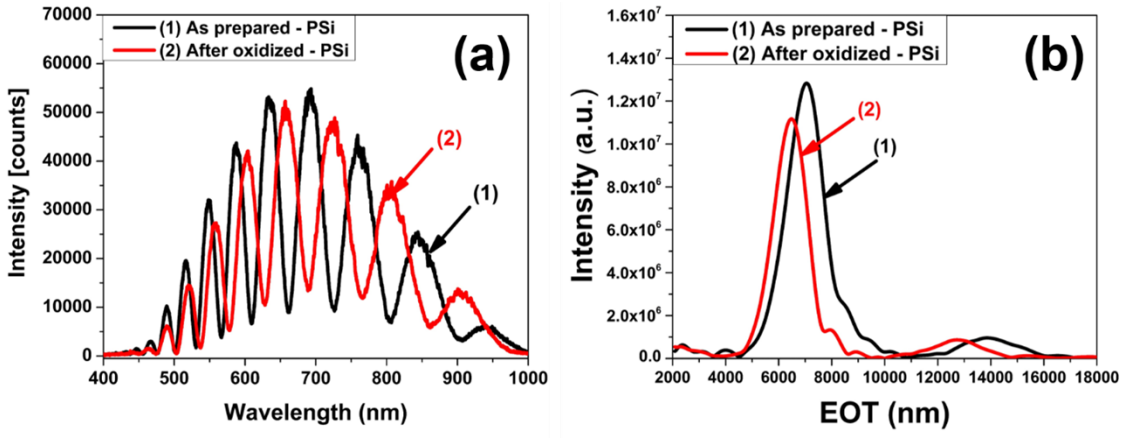

Fig. 3. Optical characterization of nanostructured PSi interferometers (a) typical reflection spectra and (b) FFT amplitude of a PSi interferometer acquired in the air before (black trace) and after (red trace).

To investigate the detection of trace metal ions in water, various aqueous solutions with NaCl concentrations ranging from 1% to 7% w/w are injected (250 μL for each concentration at 25 μL/min) into a flow cell (volume 100 μL) containing the PSi interferometers. DIW is utilized both as a solvent for the preparation of the NaCl solutions and as a carrier for infiltration of the solutions in the oxidized nanopores of the PSi interferometers. The refractive index values n_{sol} of the prepared NaCl solutions are calculated using the Lorenz-Lorentz equation [17]:

$$\frac{n_{sol}^2-1}{n_{sol}^2+2}=\sum f_i\frac{n_i^2-1}{n_i^2+2}, \tag{1}$$

where n_{sol} is the refractive index of the solution infiltrating the pores and f_i is the volume fraction of the $i^{\text{-th}}$ mixture component with refractive index n_i. Table 1 shows the refractive index variation values Δn_{sol} with different concentrations of NaCl solution.

The PSi interferometers, infiltrated with either DIW or any of the prepared NaCl solution, are characterized by calculating the average value over a wavelength of spectral interferograms, referred to as Interferogram Average over Wavelength (IAW). For each tested NaCl concentration, interferograms are obtained by subtracting the reflectance spectrum acquired after each NaCl injection from a reference reflectance spectrum acquired in DIW. All interferograms are referred to a reference interferogram calculated for DIW before initiating any NaCl injection (reference spectrum).

Table 1. The refractive index variation values Δn_{sol} with different concentrations of NaCl solution.

NaCl % (w/w)	$n_{sol,\,NaCl}$	$\Delta n_{sol,\,NaCl} = n_{sol,\,NaCl} - n_{DIW}$
0	1.333260	0
1	1.3342	0.00094
3	1.3357	0.00244
5	1.3364	0.00314
7	1.3383	0.00504

The theoretical reflectance spectra of PSi interferometers infiltrated with either DIW (reference spectrum) or with DIW containing NaCl at various concentrations are calculated as follows [15]:

$$R(\lambda) = \rho_a^2 + \rho_b^2 + 2\rho_a\rho_b\cos(\delta_{layer}) \tag{2}$$

where and are the index contrast at the filling medium-PSi and PSi-bulk silicon interfaces, respectively; is the refractive index of the filling medium,is the refractive index of bulk silicon; represents the phase delay of the interfering light beams reflected at the two interfaces, where is the PSi thickness and the wavelength.

Subtraction of the generic reflection after NaCl infiltration from the reference reflection spectrum in DIW leads to the following theoretical expression of the interferogram:

$$R - R_0 = (\rho_a^2 - \rho_{a0}^2) + (\rho_b^2 - \rho_{b0}^2) + 2[\rho_a\rho_b\cos(\delta_{PSi}) - \rho_{a0}\rho_{b0}\cos(\delta_{PSi0})] \tag{3}$$

For small variation of the refractive index values with respect to their reference values, Eq. 3 can be simplified as follows:

$$R - R_0 \cong -8\rho_{a0}\rho_{b0}\pi\Delta n_{eff}\frac{d}{\lambda}\sin(4\pi n_{eff0}\frac{d}{\lambda}) \tag{4}$$

The IAW value is eventually calculated by taking the absolute value of Eq. 4, then calculating the mean value over a sufficiently large wavelength interval centered on:

$$IAW = mean(|R - R_0|)\Big|_{\lambda_1}^{\lambda_2} \cong \frac{16d\,|\rho_{a0}\rho_{b0}|}{\lambda_0}\left|\Delta n_{eff}\right| \cdot \tag{5}$$

Here, the mean value is computed under the assumption that the $1/\lambda$ function exhibits slow variation within the wavelength range $[\lambda_1;\lambda_2]$ and can be approximated by a constant term, $1/\lambda_0$. Equation (5) emphasizes a linear correlation between the IAW value and the variation in PSi refractive index (Δn_{eff}), under the conditions where all the stated assumptions remain valid. As described by Eq. (5), PSi interferometers exhibit theoretical sensitivity to changes in the bulk refractive index of the solution infiltrating pores $\frac{16d\,|\rho_{a0}\rho_{b0}|}{\lambda_0}$, which is proportional to both the index contrasts ρ_a and ρ_b, as well as to the thickness d of the PSi, and is inversely proportional to the central wavelength (λ_0) of the selected wavelength interval used for mean value calculation.

Figure 4 illustrates the details of the IAW signal processing strategy, which involves the following main steps: (i) Record the reflection spectra in DIW (NaCl 0%) and after injection of 25 μL NaCl 7% (Fig. 4a). (ii) Obtain the reflectance spectra by normalizing the reflection

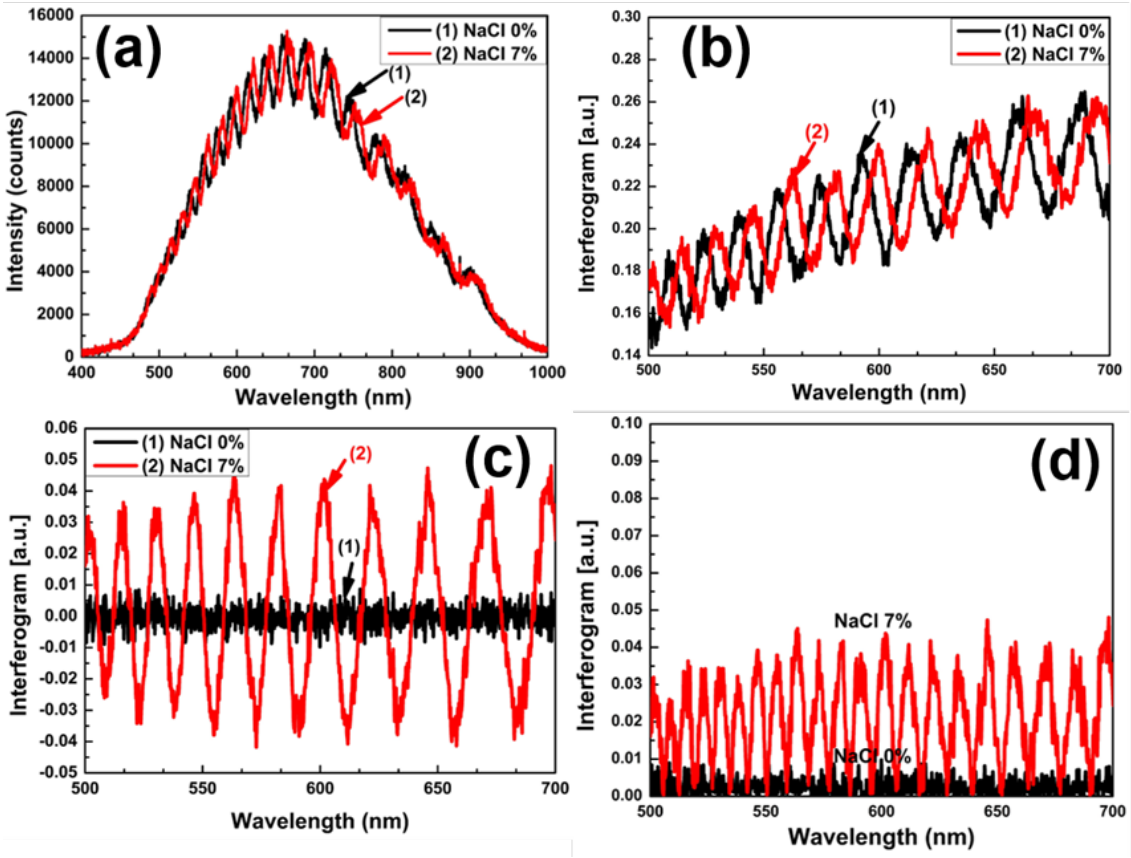

Fig. 4. Procedures for determining the IAW value for both the DIW (reference solution) and a 7% w/w NaCl solution: (a) Reflection spectra using oxidized PSi interferometers in DIW before (curve 1) and after (curve 2) infiltration of NaCl solution obtained by measurement; b) Spectral interferogram for DIW (curve 1) and NaCl solution (curve 2) by normalizing the reflection spectra with respect to a reference mirror; c) Subtraction of the intensity of the reflectance spectra obtained for the DIW infiltrated after each NaCl measurement (curve 1) and for each NaCl concentration (curve 2) from the reference spectrum d) Utilization of the absolute-value function to the interferogram in (c), then calculation of the output signal IAW is carried out by taking average of the interferogram in (d) across the wavelength spanning from 500 to 700 nm.

spectra with respect to a reference mirror over the wavelength range 500 – 700 nm (Fig. 4b). (iii) Subtract the intensity (wavelength by wavelength) of the reflectance spectra obtained for each NaCl concentration (curve 2) and for the DIW infiltrated after each NaCl measurement (curve 1) from the reference spectrum (Fig. 4c). (iv) Apply the absolute-value function to the interferogram in (c) (Fig. 4d), then compute the output signal IAW by taking average of the interferogram in (d) considering the wavelength range from 500 to 700 nm.

In Fig. 5 typical spectral interferograms obtained through the IAW reflectance spectroscopy in DIW (reference interferogram, black trace) and in (from 1% to 7% w/w corresponding to Fig. 5a

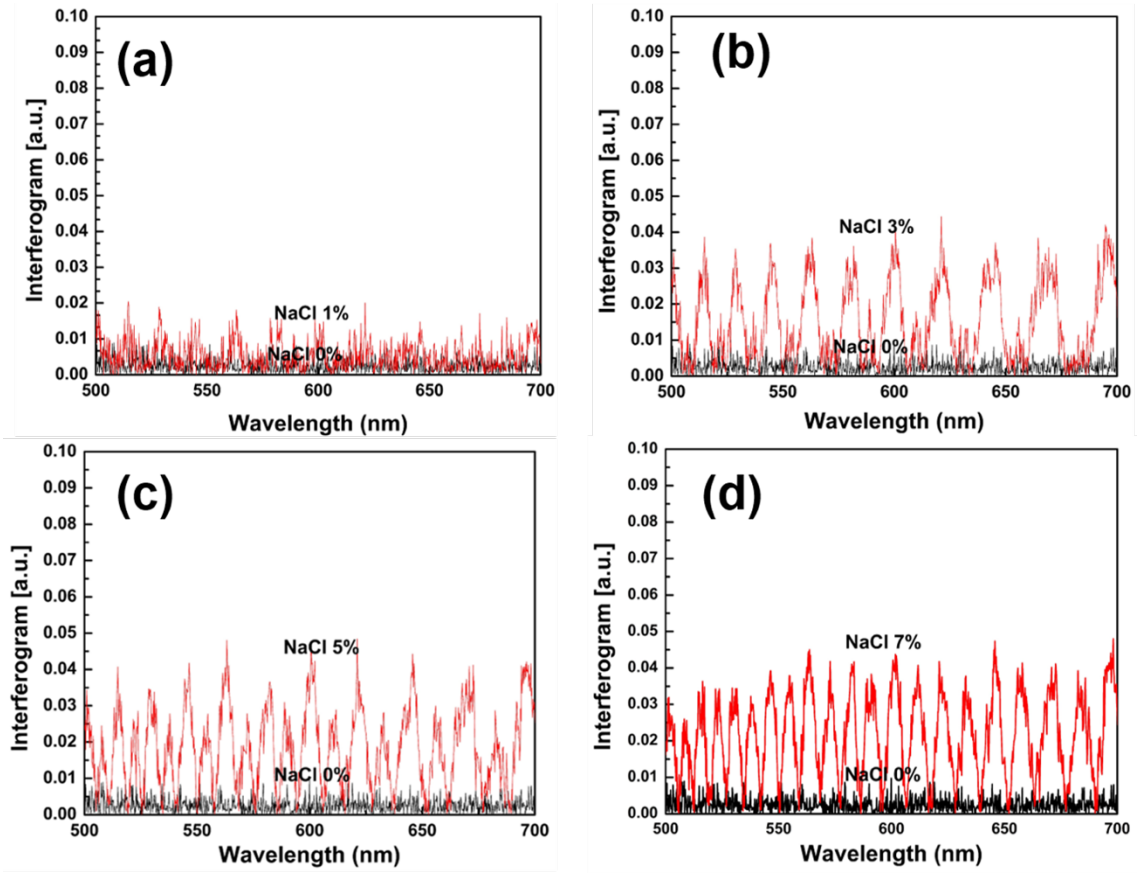

Fig. 5. Interferograms of PSi interferometers with DIW solutions with NaCl concentration of (a) 1%, (b) 3%, (c) 5% and (d) 7%.

to Fig. 5d) NaCl solutions (red trace) are shown. The reference interferogram exhibits noise spanning the entire measurement wavelength range. Notably, the interferogram from the 7% w/w NaCl solution distinctly differs from the reference, indicating the capacity to measure a refractive index variation of 5.04×10^{-3} RIU within the infiltrated nanopores with a robust signal-to-noise ratio. Accordingly, the IAW values (calculated as the average value in the interferograms in Fig. 4d over the wavelength range 500–700 nm) for DIW and for 7% w/w NaCl solution over four replicates are $IAW_0 = 0.001 \pm 0.0005$ au (blank value) and $IAW_{7\%NaCl} = 0.40276 \pm 0.00012$ au, respectively, which yield a net differential signal $-IAW_{7\%NaCl} - IAW_0 = 0.40266 \pm 0.00013$ au. The standard deviation, $\sigma_{IAW0} = 0.001$ au, establishes the experimental noise floor for the proposed PSi interferometers in DIW and enables the calculation of signal-to-noise ratio for a given NaCl solution. Impressively, a relatively high signal-to-noise ratio $S/N = IAW_{7\%NaCl}/\sigma_{IAW0} \approx 400$ is achieved for the 7% w/w NaCl solution compared to DIW, corresponding to a refractive index variation of 5.04×10^{-3} RIU within the infiltrated pores. This scale of sensitivity has been obtained in more complex structures which demand much higher costs in fabrication [12, 13].

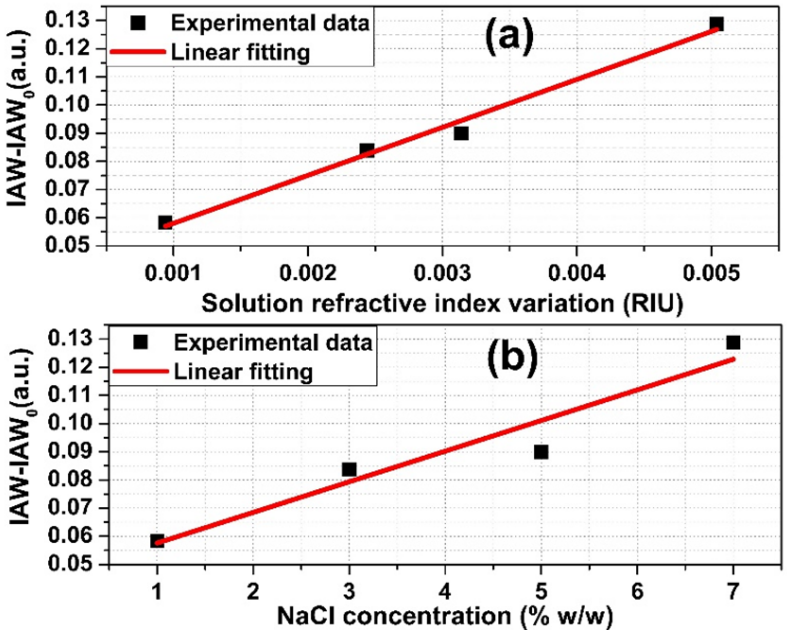

Fig. 6. Experimental calibration curve of the proposed PSi interferometers operating as optical refractive index sensors showing the output IAW-IAW0 plotted versus (a) the refractive index variation $\Delta n_{sol,\ NaCl}$ of solutions infiltrated in the nanopores and (b) %NaCl (w/w) concentration.

In Fig. 6 the experimental calibration curve of the proposed PSi interferometers operating as optical refractive index sensors is shown. Specifically, the output signal IAW-IAW$_0$ is plotted versus both equivalent refractive index variation $\Delta n_{sol,\ NaCl}$ of tested solutions (Fig. 6a) and %NaCl (w/w) concentration (Fig. 6b). A linear relationship (red trace) between IAW-IAW$_0$ and NaCl concentration is apparent with the best fitted by the following linear equation: IAW-IAW$_0$=0.01087C%$_{\mathrm{NaCl}}$ (R^2=0.983). It is apparent that a refractive index variation as small as 9.4 $\times$ 10^{-4} is reliably measured (IAW-IAW$_0$=0.05834). The experimental value agrees well with the detection limit (DL) value of 7.05×10^{-4} RIU analytically estimated from the best-fitting curve on correspondence of the $3\sigma_{\mathrm{IAW0}}$ level. This result is attributed to the accumulation of ions onto the surface of PSi subtrate. Additionally, the resolution (R) of the proposed PSi interferometer for refractometric applications is also calculated. This resolution quantifies the smallest refractive index variation (Δn_{sol}) in the infiltrating solution that can be reliably detected above the detection limit. The resolution is determined using the formula $R = 3\sigma_{NaCL}/S$, where σ_{NaCl} represents the noise level of the measured IAW_{NaCl} value when a solution with a specific NaCl concentration is introduced, and $S = dIAW/d\Delta n$ is the sensitivity of the PSi refractometer at that NaCl concentration. Sensitivity value is estimated by fitting mathematical functions to experimental calibration curves. This analysis yielded a sensitivity value (S) of 4.2 RIU^{-1}. The resolution of the proposed PSi interferometer is estimated to be approximately 7.1 $\times$ 10^{-4} RIU based on the obtained values, and this value is of the same order as the previously calculated detection limit.

The purpose of this experiment was to demonstrate that the effective refractive index alteration of Porous Silicon (PSi) primarily results from the bulk effect caused by variations in the refractive index of the infiltrating solution within the pores. The IAW value exhibits a rapid increase with increasing NaCl concentration, eventually reaching a steady-state value determined by the concentration of NaCl. Conversely, upon removal of NaCl through DIW injection, the IAW value promptly decreases and returns to the baseline observed in DIW. This observation supports our supposition that, within this concentration range, the impact of the bulk effect outweighs that of the surface effect on the variation of the effective refractive index of PSi, Δn_{eff}. Equation (5) has demonstrated that the IAW signal of a PSi interferometer can be calculated as a function of refractive index values of the solution infiltrating the pores. This equation shows that the IAW signal linearly depends on the refractive index variation of the solution infiltrating the pores.

4. Conclusion

In our study, we have successfully demonstrated experimental approaches employing facile fabrication technique by utilizing the effective electrical double layer-induced accumulation (EDL-ISA) of cations (specifically Na+) onto the negatively charged oxidized surface of PSi interferometers. This strategic application has proven to significantly enhance the performance of PSi interferometers as refractive index sensors, leading to noteworthy advancements in terms of resolution and detection limit (about of 10^{-4} RIU). We can envision that the concept of EDL-ISA holds promise for extending its efficacy to other nanostructured platforms beyond PSi. By doing so, it can effectively enhance sensitivity even in scenarios involving small refractive index variations. This extension has the potential to revolutionize the landscape of miniaturized optical refractive index sensors, introducing unprecedented levels of sensitivity, resolution, and detection limit. This progress would transcend the confines of device architecture and operating principles, marking a remarkable advancement in the field of optical refractometer miniaturization.

Acknowledgments

This work financially supported by Vietnam Academy of Science and Technology under Project No. VAST03.07/23-24.

References

[1] N. H. Maniya and D. N. Srivastava, *Fabrication of porous silicon based label-free optical biosensor for heat shock protein 70 detection*, Mater. Sci. Semicond. Process. **115** (2020) 105126.

[2] Z. A. Zaky, A. M. Ahmed, A. S. Shalaby and A. H. Aly, *Refractive index gas sensor based on the Tamm state in a one-dimensional photonic crystal: Theoretical optimisation*, Sci. Rep. **10** (2020) 9736.

[3] Z. A. Zaky, S. Alamri, V. D. Zhaketov, and A. H. Aly, *Refractive index sensor with magnified resonant signal*, Sci. Rep. **12** (2022) 13777.

[4] V. H. Pham, H. Bui, T. Van Nguyen, T. A. Nguyen, T. S. Pham, V. D. Pham, T. C. Tran, T. T. Hoang, and Q. M. Ngo, *Progress in the research and development of photonic structure devices*, Adv. Nat. Sci. Nanosci. Nanotechnol. **7** (2016) 015003.

[5] H. Bui, V. H. Pham, V. D. Pham, T. H. C. Hoang, T. B. Pham, T. C. Do, Q. M. Ngo, and T. Van Nguyen, *Determination of low solvent concentration by nano-porous silicon photonic sensors using volatile organic compound method*, Environ. Technol. **40** (2019) 3403.

[6] V. H. Pham, T. Van Nguyen, T. A. Nguyen, V. D. Pham, and H. Bui, *Nano porous silicon microcavity sensor for determination organic solvents and pesticide in water*, Adv. Nat. Sci. Nanosci. Nanotechnol. **5** (2014) 045003.

[7] F. A. Harraz, *Porous silicon chemical sensors and biosensors: A review*, Sensors Actuators B Chem. **202** (2014) 897.
[8] W. D. Sacher, Y. Lin, H. Chen, S. S. Azadeh, Z. Yong, X. Luo, H. Chua, J. C. C. Mak, A. Govdeli, A. Sharma, J. C. Mikkelsen, X. Mu, A. Stalmashonak, G.-Q. Lo and J. K. S. Poon, *An Active Visible-Light Integrated Photonics Platform on 200-mm Si*, OFC (2023) Tu3C.5
[9] Pacholski, M. Sartor, M. J. Sailor, F. Cunin and G. M. Miskelly, *Biosensing Using Porous Silicon Double-Layer Interferometers: Reflective Interferometric Fourier Transform Spectroscopy*, J. Am. Chem. Soc. **127** (2005) 11636.
[10] R. F. Balderas-Valadez, R. Schürmann, and C. Pacholski, *One Spot—Two Sensors: Porous Silicon Interferometers in Combination With Gold Nanostructures Showing Localized Surface Plasmon Resonance*, Front. Chem. **7** (2019) 593.
[11] M. P. Stewart, J. M. Buriak, *Chemical and Biological Applications of Porous Silicon Technology*, Adv. Mater. **12** (2000) 859.
[12] C. Peng, C. Yang, H. Zhao, L. Liang, C. Zheng, C. Chen, L. Qin, H. Tang, *Optical Waveguide Refractive Index Sensor for Biochemical Sensing*, Appl. Sci. **13** (2023) 3829.
[13] Z. Tu, D. Gao, M. Zhang, and D. Zhang, *High-sensitivity complex refractive index sensing based on Fano resonance in the subwavelength grating waveguide micro-ring resonator,* Opt. Express **25** (2017) 20911.
[14] M. J. Sailor, *Chemistry of Porous Silicon, In Porous Silicon in Practice:Preparation, Characterization and Applications*, Wiley-VCH Verlag GmbH & Co. KGaA, (2011) 189.
[15] S. Mariani, L. M. Strambini, and G. Barillaro, *Femtomole Detection of Proteins Using a Label-Free Nanostructured Porous Silicon Interferometer for Perspective Ultrasensitive Biosensing*, Anal. Chem. **88** (2016) 8502.
[16] J. Chapron, S. A. Alekseev, V. Lysenko, V.N. Zaitsev, D. Barbier, *Analysis of interaction between chemical agents and porous Si nanostructures using optical sensing properties of infra-red Rugate filters*, Sens. Actuators B: Chem. **120** (2007) 706.
[17] W. Heller, *Remarks on Refractive Index Mixture Rules*, J. Phys. Chem. **69** (1965) 1123.